Available online at www.sciencedirect.com

jmr&t Journal of Materials Research and Technology

journal homepage: www.elsevier.com/locate/jmrt

Original Article

Effect of oxygen on defect states of $Al_{0.4}Ga_{0.6}N$ layers grown by hydride vapor phase epitaxy

Chang Wan Ahn [a], Sungsoo Park [b,**], Eun Kyu Kim [a,*]

[a] Department of Physics and Research Institute for Convergence of Basic Sciences, Hanyang University, Seoul, 04763, Republic of Korea

[b] Department of Science Education, Jeonju University, 303 Cheonjam-ro, Wansan-gu, Jeollabuk-do, Republic of Korea

ARTICLE INFO

Article history:
Received 28 September 2021
Accepted 18 January 2022
Available online 28 January 2022

Keywords:
AlGaN
Defect states
HVPE
DLTS
Schottky diode
Oxygen effect

ABSTRACT

The defect states and electrical properties of $Al_xGa_{1-x}N$ (x = 0.4) grown by hydride vapor phase epitaxy (HVPE) were investigated. To identify the effect of incorporation of elemental O in $Al_xGa_{1-x}N$ crystals, HVPE growth of $Al_xGa_{1-x}N$ crystals was conducted with and without the flow of O_2. The crystal quality and electrical properties of the $Al_xGa_{1-x}N$ layer was analyzed by X-ray diffraction and deep level transient spectroscopy (DLTS). Schottky devices for I–V, C–V and DLTS measurement were formed using Ni/Au metal and Ti/Al metallization. Capacitance DLTS spectra showed two types of deep traps of H1 and H2 in $Al_{0.4}Ga_{0.6}N$ grown without oxygen, while H1' traps were observed in $Al_{0.4}Ga_{0.6}N$ grown with oxygen. All traps were hole-like traps with activation energies of 1.3 eV(H1), 0.59 eV(H2), and 1.2 eV(H1'). These results show that the oxygen atoms can improve the crystal quality and suppress the defect states in $Al_xGa_{1-x}N$ crystals.

1. Introduction

AlN and AlGaN have favorable properties in high thermal conductivity, mechanical strength, and radiation hardness, which show promise as new materials for semiconductors such as ultraviolet light-emitting diodes (UV-LEDs), radio frequency applications such as surface acoustic wave (SAW) devices [1–6], and field emitters [7,8]. When the Al/Ga ratio is changed in $Al_xGa_{1-x}N$, an emission spectrum is generated in the wavelength range from 210 to 365 nm [9]. However, the quantum efficiency of $Al_xGa_{1-x}N$ LED is about 3% [10]. This value is too low. To improve the performance of the device, homo-substrates must be used. However, due to the lack of AlGaN native substrates, conventional AlGaN films commonly have been grown on foreign substrates such as sapphire (α-Al_2O_3) using hydride vapor phase epitaxy(HVPE), or metal-organic chemical vapor deposition (MOCVD) [11]. In this case, the AlGaN layer exhibits a high dislocation density and point defects, which was induced by lattice mismatch and thermal expansion coefficient (TEC) differences between substrates and films [12]. These are the major causes of the decreased mobility, quantum efficiency and reliability of LEDs [13,14]. To address these issues, it is important to understand the states and origin of faults in the AlGaN epilayer. In addition, AlGaN is

* Corresponding author.
** Corresponding author.
E-mail addresses: sspark@jj.ac.kr (S. Park), ek-kim@hanyang.ac.kr (E.K. Kim).

https://doi.org/10.1016/j.jmrt.2022.01.101

the formation of native defects and their complexes, such as Al vacancy and the Al vacancy–oxygen complex which provide the electronic levels inside the band gap. These deep level centers are partly responsible for the low n-type conductivity observed in Si-doped AlN and AlGaN alloys and reduced deep ultraviolet (DUV) emission efficiency.

Understanding basic point defects and their electronic structure is crucial to further improve material quality and consequently improve the performance of AlGaN-based devices. Deep level transient spectroscopy (DLTS) is a useful method for determining the defect state in the epilayer. Using this method, the activation energy, capture cross-section, and trap density of the defect can be obtained, thereby speculating the origin of the defect.

In this paper, we study the effect of oxygen on defect states and electrical properties and the defect origin of $Al_xGa_{1-x}N$ grown by HVPE, elucidating the mechanism by which these influence the performance of an AlGaN-based device.

2. Experiment

The AlGaN layers were grown on a c-plane sapphire substrate under atmospheric pressure at 1373 K using a horizontal home-made hot wall HVPE system. Metallic Al and Ga were as used as a Group III precursors, NH_3 was chosen as a reactive gas, and N_2 was used as the carrier gas. To identify the effect of incorporation of elemental O in AlGaN crystals, one set of experiments was conducted with flowing O_2 and another set was conducted without flowing O_2 [15]. First, HCl gas, NH_3 gas, and O_2 gas were supplied to the reactor for 5 min to form the oxygen terminated surface on the sapphire substrate. This is the surface treatment stage. Next, HCl gas was reacted with liquid Ga and Al metal to form GaCl and $AlCl_3$ gas at 823 K. The NH_3, GaCl, $AlCl_3$ and O_2 gases were then fed into the growth zone to form an AlGaN layer at 1373 K. This indicates the growth stage. The V/III ratio was approximately 10. In the second experiment, an AlGaN crystal was grown under the same conditions without any intentional supply of O_2 in the whole stage. The content of x in $Al_xGa_{1-x}N$ was controlled by the flow amount of HCl gas reacting with Ga and Al metal. The thickness of the grown AlGaN crystals was about 1.5 μm for all the samples. The growth rates of AlGaN crystals with and without O_2 introduction were 15 μm/h and 30 μm/h, respectively.

In the AlGaN alloy, when the amount of Al is high, the native oxide is well formed on the surface of the AlGaN layer. Prior to metal contact deposition, to remove the native oxide on surface of the AlGaN layer, the samples were dipped in a solution of the buffer oxide etchant (BOE) and HCl:H2O (1:1). After the surface cleaning, the Ti/Al (30/70 nm) metal was deposited on the Al-face of AlGaN to form Ohmic contacts using thermal evaporation. Thereafter, it was annealed at 850 °C in N_2 ambient for 1 min [16]. The Ni/Au (50 nm/100 nm) for the Schottky contact was formed on the Al face by thermal evaporation. The schematic diagram of the $Al_xGa_{1-x}N$ Schottky device is shown in Fig. 1.

In $Al_xGa_{1-x}N$, the bandgap changes with Al mole fractions can be calculated using the following equation: [17].

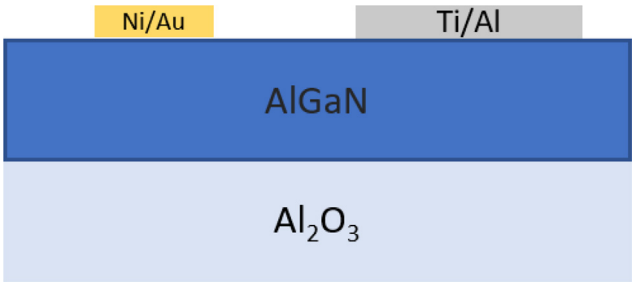

Fig. 1 – Schematic diagram of the $Al_{0.4}Ga_{0.6}N$ Schottky device.

$$E_g(x) = (1-x)E_g(GaN) + xE_g(AlN) - bx(1-x) \quad (1)$$

where $E_g(GaN)$, $E_g(AlN)$, and b are 3.5 eV, 6.1 eV, and 0.86 eV, respectively [18–20]. On the other hand, the activation energy (ΔE_a) and capture cross section (σ_n) of defect states appeared in DLTS spectra were obtained by the Arrhenius plot follow the equation [1].

$$ln\left(e_n/T^2\right) = ln\left(\sqrt{6}\,\pi 1.5k^2 m_n^* \sigma_n \Big/ h^3\right) + (-\Delta E_a / 1000k)1000 \Big/ T \quad (2)$$

Here, e_n is the emission rate, T is the measured temperature, k is the Boltzmann's constant, m^* is the effective mass, and h is the Plank's constant. Furthermore, the trap density N_t can be determined as follows:

$$N_t = 2N_d \cdot \Delta C/C \quad (3)$$

where N_d is the donor concentration, $\Delta C/C$ is the capacitance transient value of each trap peak.

To confirm the content of x in $Al_xGa_{1-x}N$ crystal, the near-band-edge (NBE) peak in photoluminescence (PL; EtaMax PLATOM) was measured at room temperature with the 213 nm wavelength. The crystal quality of the $Al_xGa_{1-x}N$ films was investigated by the (0002) X-ray omega scan rocking curve (Panalytical, X'Pert Pro MRD cradle). The DLTS measurement was performed in the temperature range of 80–600 K by a HP4280A capacitance meter and a Lake Shore 331 temperature controller. The pulse voltage (V_p) was 0 V, and measurement voltage (V_m) was −2 V. The filling pulse width was 20 ms, and the measurement interval was 50 ms.

3. Result and discussion

Fig. 2(a) shows PL spectra to measure the Al mole fraction from the bandgap. $Al_xGa_{1-x}N$ with and without oxygen has a sharp peak at 4.35 eV (~285 nm), which is called the near-band-edge(NBE) band. The increase in the bandgap of $Al_xGa_{1-x}N$ as the Al mole fractions increase. The NBE peak of $Al_xGa_{1-x}N$ obtained by Equation (1) is 4.36 eV. From this value, it can be observed that the value of x is 0.4.

High resolution X-ray diffraction (HR-XRD) was measured to determine the crystal quality of the $Al_{0.4}Ga_{0.6}N$ epilayer grown on the sapphire substrate by HVPE. The omega scan HR-XRD rocking curve for (002) planes of $Al_{0.4}Ga_{0.6}N$ epilayer

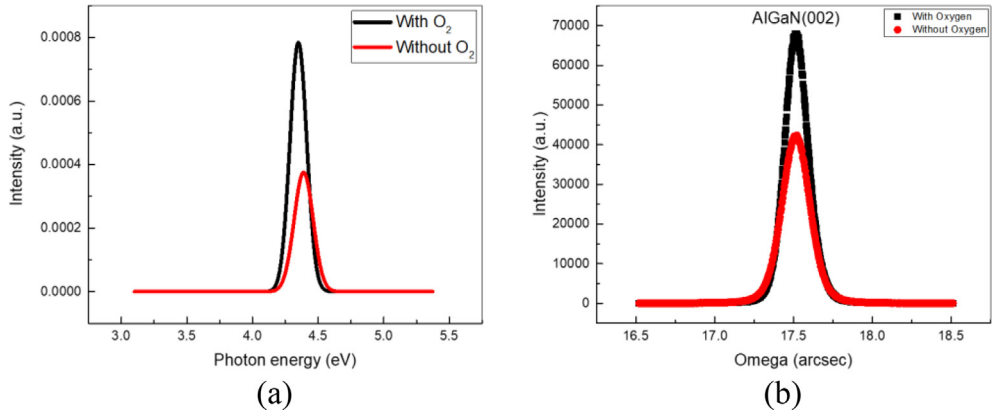

Fig. 2 – (a) Near-Band Edge of PL spectra and (b) HR-XRD rocking curve of (002) planes of the $Al_{0.4}Ga_{0.6}N$ epilayer grown with and without oxygen.

grown with and without oxygen is shown in Fig. 2(b). The full width at half maximum (FWHM) of the X-ray rocking curve for the (002) plane was compared to confirm the crystalline quality of the $Al_{0.4}Ga_{0.6}N$ epilayer with and without oxygen. The FWHM of X-ray rocking curve of $Al_{0.4}Ga_{0.6}N$ with and without oxygen were 540 arcsec and 648 arcsec, respectively. This resulted in better crystalline quality of the $Al_{0.4}Ga_{0.6}N$ epilayer, grown with oxygen. This inclination appears to be consistent with that previously reported effect of oxygen on the growth of the AlN epilayer [15].

The current–voltage(I–V) measurements of the Ni/Au $Al_{0.4}Ga_{0.6}N$ Schottky diode was performed at room temperature. Measurement was performed from 5 V to −5 V, Fig. 3 shows that the Ni/Au $Al_{0.4}Ga_{0.6}N$ Schottky diode is well-formed. In addition, the inset in Fig. 3 shows that the forward and reverse leakage currents increase exponentially with bias voltage and involve thermoelectric field emission and trap-assisted tunneling [1,21]. Furthermore, the $Al_{0.4}Ga_{0.6}N$ without oxygen is higher in leakage current at the reverse voltage than $Al_{0.4}Ga_{0.6}N$ with oxygen, it can be inferred that $Al_{0.4}Ga_{0.6}N$ without oxygen has more defects. The ideality factor at room temperature based on the I–V data of $Al_{0.4}Ga_{0.6}N$ was obtained 1.50 for grown with oxygen, and 1.89 for grown without oxygen.

Fig. 4 shows the capacitance–voltage (C–V) depth profile measured at room temperature. Measurement was performed from 0 V to −5 V. Based on the C–V measurement results(inset), we confirmed that the depletion region of the $Al_{0.4}Ga_{0.6}N$ epilayer was well-formed. The carrier concentration of the $Al_{0.4}Ga_{0.6}N$ epilayer with and without oxygen during the growth were 1.97×10^{17} cm^{-3}, 6.29×10^{16} cm^{-3}, and the Schottky barrier height of the $Al_{0.4}Ga_{0.6}N$ epilayer with and without oxygen was 1.00 eV and 1.01 eV, respectively. The difference in carrier concentration between the $Al_{0.4}Ga_{0.6}N$ epilayer with and without oxygen seems to be the effect of oxygen spilled during growth. The fact that the carrier concentration of the $Al_{0.4}Ga_{0.6}N$ epilayer with oxygen is higher than the $Al_{0.4}Ga_{0.6}N$ epilayer without oxygen is in good agreement with oxygen acting as an n-type dopant.

Fig. 5 shows the DLTS signal an emission rate of 5.12 Hz and the Arrhenius plot(inset). DLTS signal of $Al_{0.4}Ga_{0.6}N$ epilayer with oxygen (Fig. 5(a)) shows a hole like trap near 400 K (H1′). The H1 (460 K) and H2 (350 K) traps were obtained from $Al_{0.4}Ga_{0.6}N$ epilayer without oxygen(Fig. 5(b)). The H1 and H1′ traps have similar activation energies and capture cross sections. The parameters of deep levels were obtained by using the Equation (2), and then the activation energy of H1 and H1′ are 1.3 ± 0.05 eV and 1.2 ± 0.05 eV, respectively. The capture

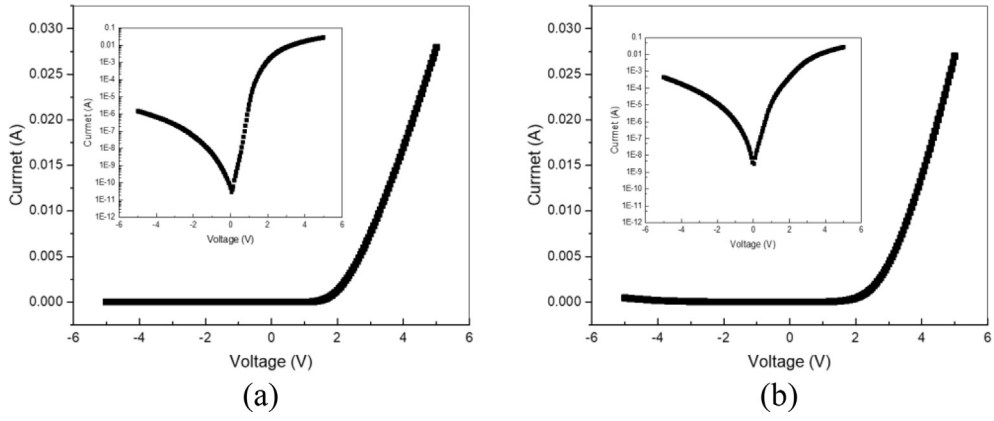

Fig. 3 – I–V Characteristic of the Ni/Au/AlGaN Schottky diode at room temperature. (a) $Al_{0.4}Ga_{0.6}N$ with oxygen, (b) $Al_{0.4}Ga_{0.6}N$ without oxygen.

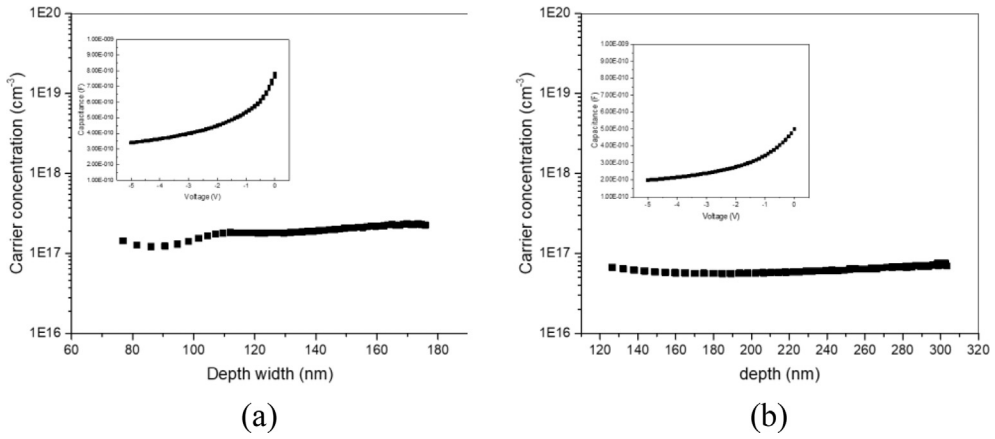

Fig. 4 – C–V Characteristic and depth profile of the $Al_{0.4}Ga_{0.6}N$ epilayer (a) with oxygen, (b) without oxygen.

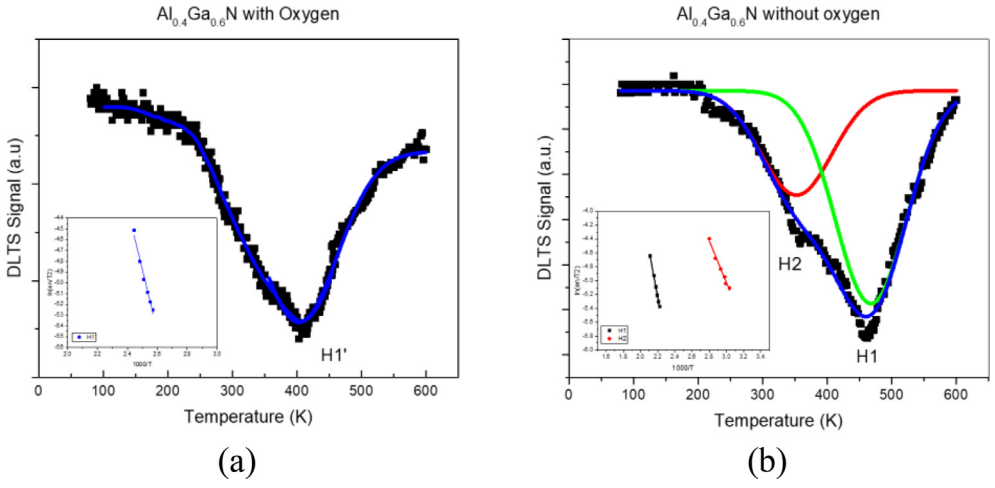

Fig. 5 – DLTS signal and Arrhenius plot(inset) of the $Al_{0.4}Ga_{0.6}N$ epilayer (a) with oxygen, (b) without oxygen.

Table 1 – Deep level parameters measured from the $Al_{0.4}Ga_{0.6}N$ epilayer.

Sample	Carrier traps	Activation energy (eV)	Capture Cross Section (cm^2)	Trap density (cm^{-3})
$Al_{0.4}Ga_{0.6}N$ with oxygen	H1′	1.2 ± 0.05	3.37×10^{-13}	1.82×10^{14}
$Al_{0.4}Ga_{0.6}N$ without oxygen	H1	1.3 ± 0.05	4.45×10^{-13}	1.25×10^{15}
	H2	0.59 ± 0.01	1.47×10^{-18}	7.95×10^{14}

cross section of H1 and H1′ are 4.45×10^{-13} cm^2, and 3.37×10^{-13} cm^2, respectively. The activation energy of H2 is 0.59 ± 0.01 eV above the valence band edge. The capture cross section of H2 is 1.47×10^{-18} cm^2. The density for each trap was calculated as 1.25×10^{15}(H1), 7.95×10^{14}(H2), and 1.82×10^{14}(H1') cm^{-3}, respectively, by the Equation (3). The defect states are summarized in Table 1.

In general, the point defect is easily produced as the Al mole fraction of $Al_xGa_{1-x}N$ increases, and the origin is from the cation vacancies (V_{III}) or related complex [22,23]. The origin of the trap H1 and H1′ is the native cation(group III sublattice) vacancy(V_{III}) such as V_{Ga} and V_{Al} [24,25] or V_{III}-$O_N^{2-/1-}$ [26,27], and the H2 origin seems to be V_{III}-$2O_N^{1-/0}$ [26–28]. The defect measurement results were compared with or without oxygen flow during growth of the $Al_{0.4}Ga_{0.6}N$ epilayer. The additional H2 trap was only observed in the $Al_{0.4}Ga_{0.6}N$ epilayer without oxygen, and this defect is believed to have disappeared from the $Al_{0.4}Ga_{0.6}N$ with the oxygen sample due to the oxygen spillage during $Al_{0.4}Ga_{0.6}N$ epilayer growth. Further research is needed to determine how the H1' defect in the $Al_{0.4}Ga_{0.6}N$ epilayer with oxygen during growth will affect the device.

4. Conclusion

We investigated the crystal quality and defect states in $Al_xGa_{1-x}N$ based Schottky diodes to identify the effect of incorporation of oxygen in $Al_xGa_{1-x}N$ crystals. It is confirmed that the Al

mole fractions of the $Al_xGa_{1-x}N$ crystal is 0.4 from the value of the NBE peak in the PL spectrum. We can verify that the crystal quality the $Al_{0.4}Ga_{0.6}N$ epilayer with oxygen was better than that without oxygen from the XRD data. The defect states were investigated by DLTS, and there are three types of a hole-like trap in the device. The activation energy of each trap is 1.3 ± 0.05 eV (H1), 1.2 ± 0.05 eV (H1′), and 0.59 ± 0.01 eV (H2). Capture cross sections of the trap are 4.45×10^{-13} cm^2 (H1), 3.37×10^{-13} cm^2 (H1′), and 1.47×10^{-18} cm^2 (H2), respectively. Additionally, each trap density is 1.25×10^{15} cm^{-3} (H1), 7.95×10^{14} cm^{-3} (H2), and 1.82×10^{14} cm^{-3} (H1′).The trap origin of H1 and H1′ is the V_{Al}-V_O complex or V_{III}-O_N and the origin of H2 is V_{III}-$2O_N$. The H2 trap has been further observed in the $Al_{0.4}Ga_{0.6}N$ epilayer grown without oxygen, and this defect was disappeared by oxygen spilling during growth. As a result, the defect concentration was reduced, and the crystal quality was improved. In conclusion, the O2 flow used for $Al_xGa_{1-x}N$ growth reduced the deep level center. Further research is needed to determine the mechanism by which the H1' defect in the $Al_{0.4}Ga_{0.6}N$ epilayer with oxygen during growth will affect the device.

Declaration of Competing Interest

The authors declare that they have no known competing financial interests or personal relationships that could have appeared to influence the work reported in this paper.

Acknowledgements

This research was supported in part by the Basic Science Research Program through the National Research Foundation of Korea (NRF) funded by the Ministry of Education (No. 2018R1D1A1B07042909), and by the NRF grant funded by the Korean government (MSIT) (NRF-2020R1A4A4078674).

REFERENCES

[1] Lee M, Ahn CW, Vu TKO, Lee HU, Kim EK, Park S. First observation of electronic trap levels in freestanding GaN crystals extracted from Si substrates by hydride vapour phase epitaxy. Sci Rep 2019;9:7128.
[2] Lee M, Ahn CW, Vu TKO, Lee HU, Jeong Y, Hahm MG, et al. Current transport mechanism in palladium Schottky contact on Si-based freestanding GaN. Nanomaterials 2020;10:297.
[3] Shih H-Y, Shiojiri M, Chen C-H, Yu S-F, Ko C-T, Yang J-R, et al. Ultralow threading dislocation density in GaN epilayer on near-strain-free GaN compliant buffer layer and its applications in hetero-epitaxial LEDs. Sci Rep 2015;5:13671.
[4] Jaros A, Hartmann J, Zhou H, Szafranski B, Strassburg M, Avramescu A, et al. Photoluminescence of planar and 3D InGaN/GaN LED structures excited with femtosecond laser pulses close to the damage threshold. Sci Rep 2018;8:11560.
[5] DuChene JS, Tagliabue G, Welch AJ, Cheng W-H, Atwater HA. Hot hole collection and photoelectrochemical CO 2 reduction with plasmonic Au/p-GaN photocathodes. Nano Lett 2018;18:2545–50.
[6] Chung K, Beak H, Tchoe Y, Oh H, Yoo H, Kim M, et al. Growth and characterizations of GaN micro-rods on graphene films for flexible light emitting diodes. Apl Mater 2014;2:092512.
[7] Li D, Jiang K, Sun X, Guo C. AlGaN photonics: recent advances in materials and ultraviolet devices. Adv Opt Photon 2018;10:43.
[8] Northrup JE, Chua CL, Yang Z, Wunderer T, Kneissl M, Johnson NM, et al. Effect of strain and barrier composition on the polarization of light emission from AlGaN/AlN quantum wells. Appl Phys Lett 2012;100:021101.
[9] Fukuyo F, Ochiai S, Miyake H, Hiramatsu K, Yoshida H, Kobayashi Y. Growth and characterization of AlGaN multiple quantum wells for electron-beam target for deep-ultraviolet light sources. Jpn J Appl Phys 2013;52:01AF03.
[10] Khan MA, Matsumoto T, Maeda N, Kamata N, Hirayama H. Improved external quantum efficiency of 293 nm AlGaN UVB LED grown on an AlN template. Jpn J Appl Phys 2019;58:SAAF01.
[11] Wu Yi-Feng, Kapolnek D, Ibbetson JP, Parikh P, Keller BP, Mishra UK. Very-high power density AlGaN/GaN HEMTs. IEEE Trans Electron Dev 2001;48:586–90.
[12] Polyakov AY, Lee I-H. Deep traps in GaN-based structures as affecting the performance of GaN devices. Mater Sci Eng R Rep 2015;94:1–56.
[13] Lee SR, West AM, Allerman AA, Waldrip KE, Follstaedt DM, Provencio PP, et al. Effect of threading dislocations on the Bragg peakwidths of GaN, AlGaN, and AlN heterolayers. Appl Phys Lett 2005;86:241904.
[14] Ma Z, Almalki A, Yang X, Wu X, Xi X, Li J, et al. The influence of point defects on AlGaN-based deep ultraviolet LEDs. J Alloys Compd 2020;845:156177.
[15] Lee M, Yang M, Lee H-Y, Lee HU, Kim H, Park S. High crystalline aluminum nitride via highly enhanced adatom diffusion driven by point defect complex. Appl Surf Sci 2020;505:144615.
[16] Qiao D, Yu LS, Lau SS, Redwing JM, Lin JY, Jiang HX. Dependence of Ni/AlGaN Schottky barrier height on Al mole fraction. J Appl Phys 2000;87:801–4.
[17] Kuokstis E, Sun WH, Shatalov M, Yang JW, Asif Khan M. Role of alloy fluctuations in photoluminescence dynamics of AlGaN epilayers. Appl Phys Lett 2006;88:261905.
[18] Shan W, Ager JW, Yu KM, Walukiewicz W, Haller EE, Martin MC, et al. Dependence of the fundamental band gap of AlxGa1−xN on alloy composition and pressure. J Appl Phys 1999;85:8505–7.
[19] Lee SR, Wright AF, Crawford MH, Petersen GA, Han J, Biefeld RM. The band-gap bowing of AlxGa1−xN alloys. Appl Phys Lett 1999;74:3344–6.
[20] Nam KB, Li J, Nakarmi ML, Lin JY, Jiang HX. Unique optical properties of AlGaN alloys and related ultraviolet emitters. Appl Phys Lett 2004;84:5264–6.
[21] Lee M, Vu T, Lee K, Kim E, Park S. Electronic transport mechanism for Schottky diodes formed by Au/HVPE a-plane GaN templates grown via in situ GaN nanodot formation. Nanomaterials 2018;8:397.
[22] Bradley ST, Goss SH, Brillson LJ, Hwang J, Schaff WJ. Deep level defects and doping in high Al mole fraction AlGaN. J Vac Sci Technol, B 2003;21:2558.

[23] Henry TA, Armstrong A, Allerman AA, Crawford MH. The influence of Al composition on point defect incorporation in AlGaN. Appl Phys Lett 2012;100:043509.
[24] Arehart AR, Allerman AA, Ringel SA. Electrical characterization of n-type Al0.30Ga0.70N Schottky diodes. J Appl Phys 2011:11.
[25] Laaksonen K, Ganchenkova MG, Nieminen RM. Vacancies in wurtzite GaN and AlN. J Phys Condens Matter 2009;21:015803.
[26] Sedhain A, Lin JY, Jiang HX. Nature of optical transitions involving cation vacancies and complexes in AlN and AlGaN. Appl Phys Lett 2012;5.
[27] Nam KB, Nakarmi ML, Lin JY, Jiang HX. Deep impurity transitions involving cation vacancies and complexes in AlGaN alloys. Appl Phys Lett 2005;4.
[28] Nepal N, Nakarmi ML, Lin JY, Jiang HX. Photoluminescence studies of impurity transitions in AlGaN alloys. Appl Phys Lett 2006;4.